ADVANCED OPTICAL MATERIALS
www.advopticalmat.de

Surface Structure Dependent Circular Dichroism in Single and Double Gyroid Metamaterials

*Bryan M. Cote, William R. Lenart, Christopher J. Ellison, and Vivian E. Ferry**

Gyroid optical metamaterials consist of triply periodic chiral networks that are attractive photonic structures due to the combination of intriguing optical properties and spontaneous self-assembly-based fabrication routes using materials such as block copolymers. A previous experimental investigation found that gyroid metamaterials support strong circular dichroism, beyond what simulations only considering bulk interactions predict. In this work, simulations are used to unravel the contributions of bulk and surface interactions on the circular dichroism spectra of silver-infilled gyroid metamaterial films. It is found that surface interactions have a significant, often dominating, contribution to circular dichroism. The relative strength of bulk and surface contributions can be tuned by controlling the crystallographic orientation, termination plane of the film, thickness, metal volume fraction, and defect density. Importantly, the dominance of surface interactions allows double gyroids, which are achiral in the bulk, to support strong circular dichroism responses with *g*-factor magnitudes as large as 0.25.

1. Introduction

The interaction between light and gyroid structures is of interest for many emerging optical applications in photonic crystals, metamaterials, and topological photonics.[1–4] The single gyroid, with space group $I4_132$, is a triply periodic, cubic, chiral structure that contains screw axes that propagate along the crystal's principle crystallographic directions, and the achiral double gyroid, with space group $Ia\bar{3}d$, is composed of two interpenetrating single gyroid networks. Intriguingly, these gyroid structures have also been found to occur naturally: single gyroids have been identified in the wings of several butterfly[5–7] and bird[8] species and double gyroids in the retinas of tree shrews,[9] providing optical functionality such as structural colors, multifocal lenses, and UV-filtration. Optical properties of interest in gyroids include circular dichroism (CD), Kuhn's dissymmetry factor,[10] and polarization-selective reflection and transmission.

3D, chiral metamaterials are often fabricated in complex and intensive processes such as two-photon direct laser writing or multilayer electron-beam lithography.[11,12] In contrast to these top down fabrication techniques, block copolymer self-assembly and templating holds promise for large scale gyroid fabrication, producing macroscale structures with subwavelength and tunable periodicities, typically on the order of 10 s of nanometers.[13,14] At specific composition windows, triblock copolymers self-assemble into an alternating gyroid structure, consisting of two single gyroid networks surrounded by a matrix. Plasmonic, single gyroid metamaterials can then be created through the selective removal of one of the network structures, followed by infilling with a plasmonic metal as depicted in **Figure 1**a.[15–17] The resonant behavior of these plasmonic structures can therefore be tuned by typical parameters for plasmonic structures, including the unit cell dimensions, infilling fraction, and refractive index contrast with the surrounding medium.

Previous theoretical investigation into the resonant properties of single gyroid metamaterials found that they support chiral modes along the ⟨100⟩ and ⟨111⟩ families of directions.[18] Unfortunately, these modes were predicted to only support low levels of CD due to the connectivity of the screw axes within the single gyroid structure. More recently, however, there is experimental evidence that silver infilled single gyroid metamaterials exhibit strong circular dichroism in the visible and near-infrared (NIR).[19] This, combined with evidence that the linear dichroism observed in single gyroid metamaterials can be attributed to resonances on the gyroid's top surface,[20] suggests that surface resonances may also significantly contribute to a gyroid metamaterial's overall chiral optical response, in addition to the resonant interactions with the bulk that have been previously investigated. Many emerging applications of gyroid metamaterials will utilize thin films, which are naturally terminated with specific surface structures. This presents an opportunity for tuning the properties of gyroid metamaterials: as we show in this manuscript using finite-difference time-domain (FDTD) simulations, the surface orientation, thickness of the metamaterial, excitations on the front and rear surfaces, and surface defects all emerge as strategies to tune the optical

B. M. Cote, W. R. Lenart, C. J. Ellison, V. E. Ferry
Department of Chemical Engineering and Materials Science
University of Minnesota
421 Washington Ave SE, Minneapolis MN 55455, USA
E-mail: veferry@umn.edu

The ORCID identification number(s) for the author(s) of this article can be found under https://doi.org/10.1002/adom.202200363.

DOI: 10.1002/adom.202200363

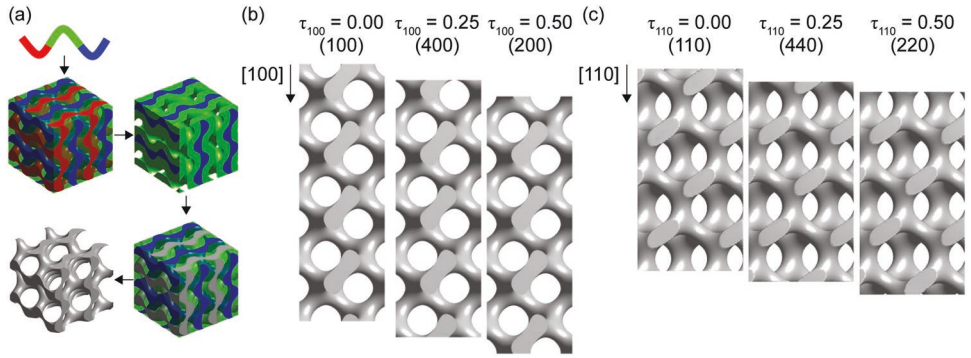

Figure 1. a) General fabrication scheme of a silver infilled single gyroid metamaterial. Effects of the termination parameter, τ_{hkl}, on the modeled volume and surface planes of a b) 4*a* thick [100] oriented gyroid and c) $2\sqrt{2}a$ thick [110] oriented gyroid.

response of gyroid metamaterials. Moreover, structures that are achiral in the bulk but chiral on the surface also exhibit circular dichroism, extending the versatility of this system.

2. Results and Discussion

We first show a few selected examples that demonstrate that the CD spectra of the gyroid metamaterials change dramatically with different termination planes. **Figure 2**a shows examples of the calculated CD spectra for [100] oriented single gyroid metamaterials terminated at the (100) or (800) planes, corresponding to [100] termination coordinates (τ_{100}) of 0 or 0.125, respectively, as described in Section 4. All gyroids have a unit cell length (*a*) of 65 nm, are 260 nm (4*a*) thick, and consist of ≈20 vol% silver in air ($|m| = 0.9$), as defined by Equation (4) in the Experimental Section. Both positive ($m = +0.9$) and negative ($m = -0.9$) single gyroid networks are considered. While all the [100] oriented gyroids exhibit a feature in the CD spectrum at ≈500 nm whose sign depends on the sign of the gyroid, the (100) terminated gyroids ($\tau_{100} = 0$) also support an additional CD feature at 584 nm. It is important to note that in general the wavelengths where the absorption is maximized are not necessarily the same as the CD peaks. In this study, all CD peaks correlate with absorption maxima but are often slightly red- or blue-shifted, as observed in Figure S1 of the Supporting Information.

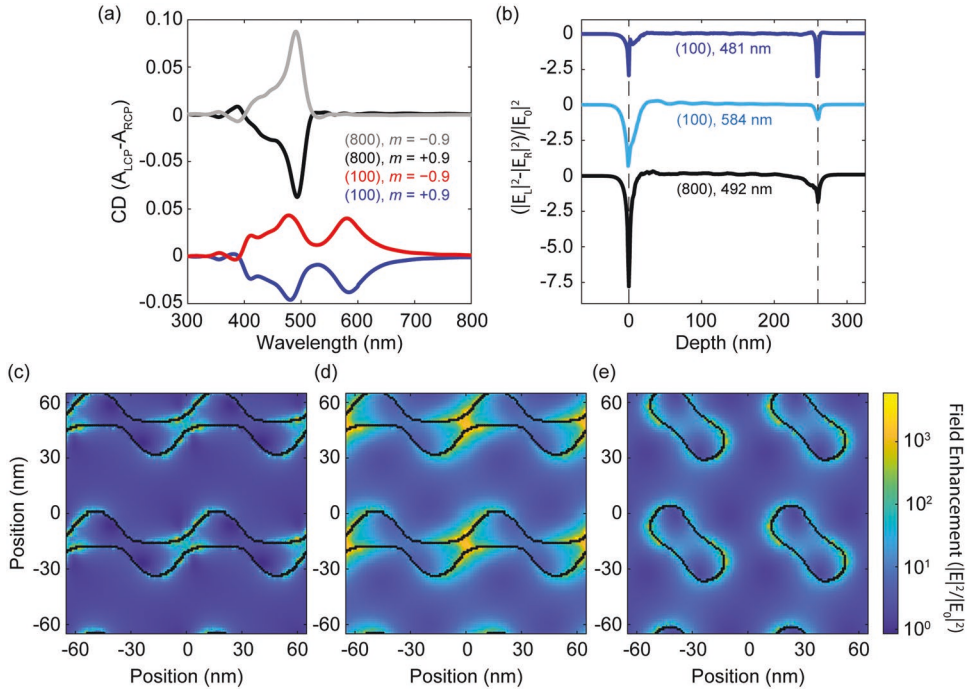

Figure 2. a) Circular dichroism spectra of 260 nm thick (4*a*) [100] oriented single gyroid metamaterials with ≈20 vol% Ag fill ($m = \pm 0.9$) and different terminations. b) Integrated difference in electric field intensity enhancement around the positive gyroids at the CD peaks through the depth of the gyroid structure. Dashed lines indicate the top and bottom termination planes. c,d) Top view of the unpolarized electric field enhancement at the top surface of the positive ($m = +0.9$) gyroids. (c) (100) terminated ($\tau_{100} = 0$) at $\lambda = 481$ nm, (d) (100) terminated ($\tau_{100} = 0$) at $\lambda = 584$ nm, e) (800) terminated ($\tau_{100} = 0.125$) at $\lambda = 492$ nm. The black outline indicates the Ag–air interface.

To show that these different CD spectra result from differences in the surface termination, we examine the electric fields both through the depth of the gyroid film and at the surface. Figure 2b shows the integrated difference between the electric field intensity enhancement under left- and right-handed circularly polarized light as a function of depth through the positive (m = +0.9) single gyroid structures. The integrated difference in electric field intensity enhancement is calculated using Equation (1)

$$\frac{\Delta I}{I_0}(x) = \frac{\int\left[\left|E_{\mathrm{LCP}}(x)\right|^2 - \left|E_{\mathrm{RCP}}(x)\right|^2\right] \mathrm{d}A}{\int\left|E_0\right|^2 \mathrm{d}A} \tag{1}$$

where A defines the plane perpendicular to light propagation at a depth of x below the top termination plane. The area integrations are performed over the entire plane between the periodic boundary conditions within the simulation region. $|E_{\mathrm{LCP,\ RCP}}(x)|^2$ is the electric field intensity at that plane due to LCP or RCP illumination, and $|E_0|^2$ is the intensity of the incident plane wave source. A depth of 0 nm corresponds to the top surface, and 260 nm is the bottom termination of the gyroid film. At the wavelengths of the CD peaks, the electric field intensity differences are concentrated at the surfaces of the gyroids. At the wavelengths of the CD peaks, the electric field intensity differences are concentrated at the surfaces of the gyroids. The unpolarized electric field intensity enhancement at the top surfaces at the CD peaks is shown in Figure 2c–e. The electric field intensity enhancement at the bottom surfaces is included in Figure S2 of the Supporting Information. There are notably negligible selective interactions within the bulk of these [100] oriented single gyroid metamaterials. While single gyroids have screw axes along the [100] direction, providing chirality to the bulk,[21] the connectivity of these helical screw axis and the presence of two screw axes of opposite handedness along the [100] direction lead to a decreased chiral optical response within the bulk.[18] Analysis of additional CD peaks presented in Figure S3 of the Supporting Information shows that all CD peaks, except for the small CD peaks at ≈355 nm, have significant contributions from the top and bottom surfaces.

The structural symmetry of the termination dependent circular dichroism of the single gyroid is observed when we expand our search to encompass all possible surface groups along the [100] direction. **Figure 3**a,b shows the termination resolved circular dichroism spectra for both positive (m = +0.9) and negative (m = –0.9) silver gyroid metamaterials, respectively, oriented along [100]. Schematics of the surface groups for the

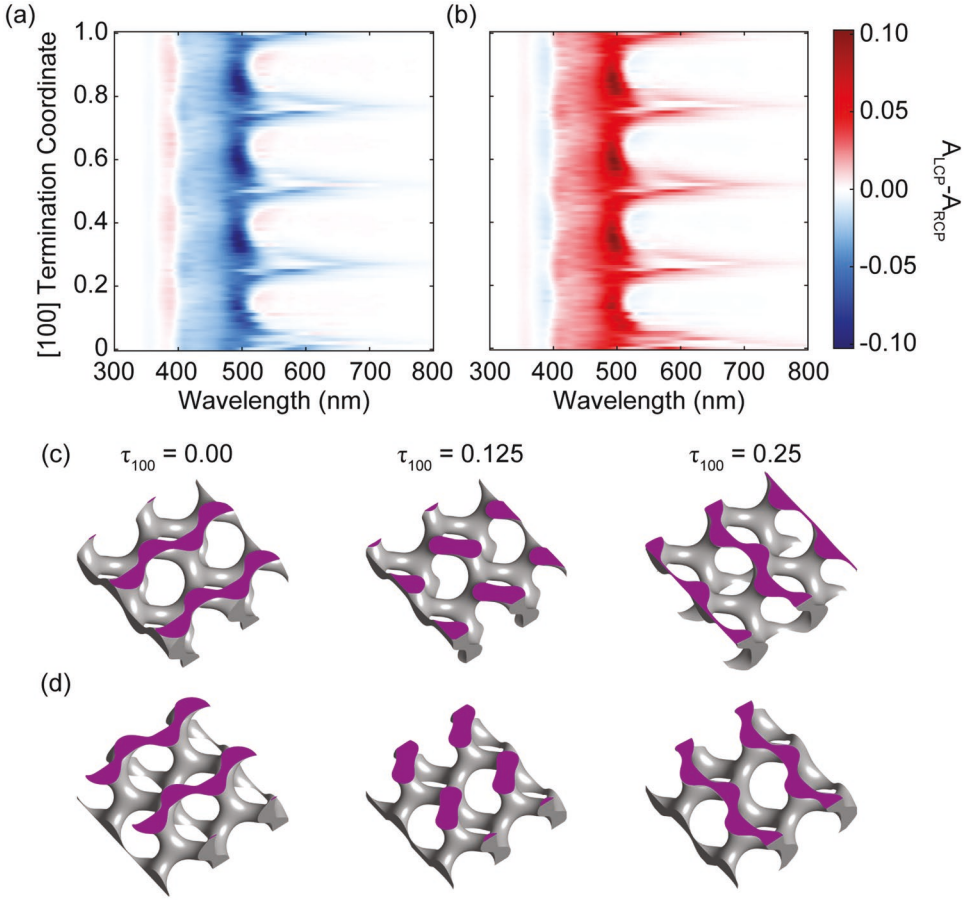

Figure 3. Termination dependent circular dichroism for 260 nm thick (4*a*) [100] oriented a) positive (m = +0.9) and b) negative (m = –0.9) gyroid metamaterials for all possible surface groups. Schematics of the top surface of the c) positive and d) negative single gyroid metamaterials for different terminations along the [100] direction. The termination planes are colored purple for improved visibility.

two single gyroid networks are shown in Figure 3c,d to highlight the enantiomeric structure of the two single gyroids. The 4_1 screw axis along the single gyroid's ⟨100⟩ family of directions results in a periodic termination dependent profile that repeats every $\Delta\tau_{100} = 0.25$ with red-shifted CD spectrum peaks of opposite handedness occurring at (100), (400), and (200) termination planes, corresponding to [100] termination coordinates of 0, 0.25 (and 0.75), and 0.5, respectively. These red-shifted CD peaks are due to the creation of identical thinly connected "S" shaped top surfaces. In between these "S" shaped termination groups, the gyroid's top surface consists of square arrays of more isolated nanorod arrays that selectively interact with left- or right-handed circularly polarized light depending on the handedness of the 4_1 screw.

Decomposition of the CD spectrum into its constituent components, the difference in circularly polarized reflectance and transmittance, provides further insight into the chiral optical behavior of these [100] oriented single gyroids. Figure S4 of the Supporting Information shows that the CD is largely only detectable in transmittance, with the difference in left and right handed circularly polarized transmittance approximately five times larger than that observed in reflectance measurements. These results agree with the findings in Figure 2b where the bottom surfaces also selectively concentrate light of a single handedness.

An important figure of merit for chiral optical devices is the Kuhn's dissymmetry factor, g,[10,22] given by the following expression

$$g = \frac{(A_L - A_R)}{\frac{1}{2}(A_L + A_R)} \tag{2}$$

These gyroids have g-factors on the order of ±0.18 (Figure S5, Supporting Information), orders of magnitude larger than many chiral molecules, and large enough for gyroid metamaterials to be promising candidates for many chiral optical applications.[23]

The contrasting effects of bulk and surface resonances can be more easily observed by rotating the [100] oriented gyroids 45° to access the [110] direction. The termination dependent CD spectra of the positive ($m = +0.9$) and negative ($m = -0.9$) single gyroids are shown in **Figure 4**a,b. In this orientation, both termination independent and termination dependent CD spectra are observed. The termination independent CD spectra contain both positive and negative CD peaks centered at ≈400 nm indicative of the Cotton effect. We note that slight differences are still observed with termination. The termination dependent CD spectra are red-shifted relative to the termination independent signal and are observed in the positive ($m = +0.9$) gyroid at a τ_{110} range from 0.12 to 0.44, and in the negative ($m = -0.9$)

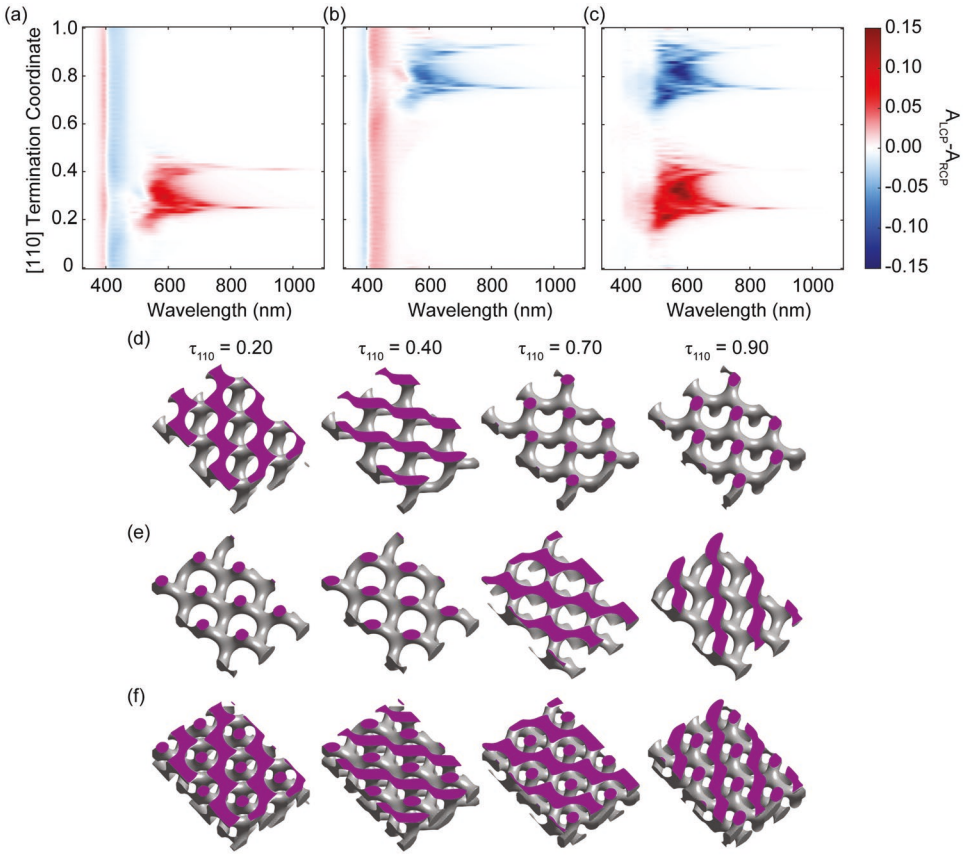

Figure 4. Termination resolved circular dichroism spectra for 368 nm thick ($4\sqrt{2}a$) [110] oriented a) positive ($m = +0.9$) and b) negative ($m = -0.9$) single gyroid metamaterials and c) double gyroids ($m = \pm 0.9$). Schematics of the top surface of the d) positive and e) negative single gyroids and f) double gyroids for different terminations along the [110] direction. The termination planes are highlighted in purple for improved visibility.

gyroid at a termination range of 0.62 to 0.94, corresponding to a $\Delta\tau_{110} = 0.5$ shift in enantiomeric CD response.

The $\Delta\tau_{110} = 0.5$ shift in enantiomeric CD response between the two single gyroid networks is explained by the interweaving of the two single gyroid networks along the [110] direction. Schematics for the surface groups both close to and far from these termination dependent CD peaks are shown in Figure 4d–f. When one single gyroid network has the desired termination groups to create a particular surface resonance, the top surface of the other network does not generate the mirror image structure. Instead, the other network fills in the gaps, forming a hexagonally packed cylinder arrangement that cannot generate the same chiral surface resonances. The enantiomeric equivalent surface is located in the other single gyroid network $\Delta\tau_{110} = 0.5$ away.

The origin of these termination independent and termination dependent CD spectral features can be confirmed by investigating their local electric fields, as shown in Figure S6 of the Supporting Information. The termination dependent CD signal is generated by chiral surface resonances that occur when the top surface of the single gyroid metamaterial concentrates electric fields, identical to the structures reported to lead to linear dichroism in gyroid metamaterials.[20] The termination independent CD signal, on the other hand, is generated by bulk interactions, as observed by the preferential concentration, and in turn attenuation, of one circular polarization throughout the entire metamaterial in Figure S6b,d of the Supporting Information. The termination independent CD is only detectible in transmittance measurements, as these bulk effects occur as light travels through the bulk of the gyroid metamaterial (Figure S7, Supporting Information). By contrast, the termination dependent, surface driven CD is primarily detectable in reflectance measurements.

This $\Delta\tau_{110} = 0.5$ shift in enantiomeric response between the positive ($m = +0.9$) and negative ($m = -0.9$) single gyroid networks enables double gyroids, a metamaterial design not previously considered for chiral optical applications, to generate strong CD signals. Figure 4c shows that the termination dependent CD response for a [110] oriented gyroid double gyroid that is formed by infilling both the positive and negative single gyroid networks with silver. Infilling both networks forms a metamaterial that is achiral in the bulk and therefore lacks any bulk contributions to the CD signal. However, the $\Delta\tau_{110} = 0.5$ displacement in surface driven chiral optical responses of the two constituent single gyroid networks allows for double gyroids to support surface driven CD responses, resulting in a metamaterial that generates strong positive and negative CD spectra depending on the termination plane selected. Furthermore, the double gyroid's CD responses are found to be enhanced compared to the single gyroid constituents in both strength and g-factor ($|g_{single}| = 0.16$ vs $|g_{double}| = 0.25$).

Since we have seen that much of the CD signal arises from the top interface, it is important to determine whether the bulk of the single gyroid system is even necessary to support the red-shifted resonances. We compare the electric field intensity profiles, the integrated difference in electric field intensity enhancement, and the resulting CD of a multiunit cell thick (368 nm, or $4\sqrt{2}a$) gyroid metamaterial film that supports both surface and bulk interactions to a gyroid metasurface that is too thin to support bulk CD (23 nm, or $\sqrt{2}/4a$) (**Figure 5**). We note

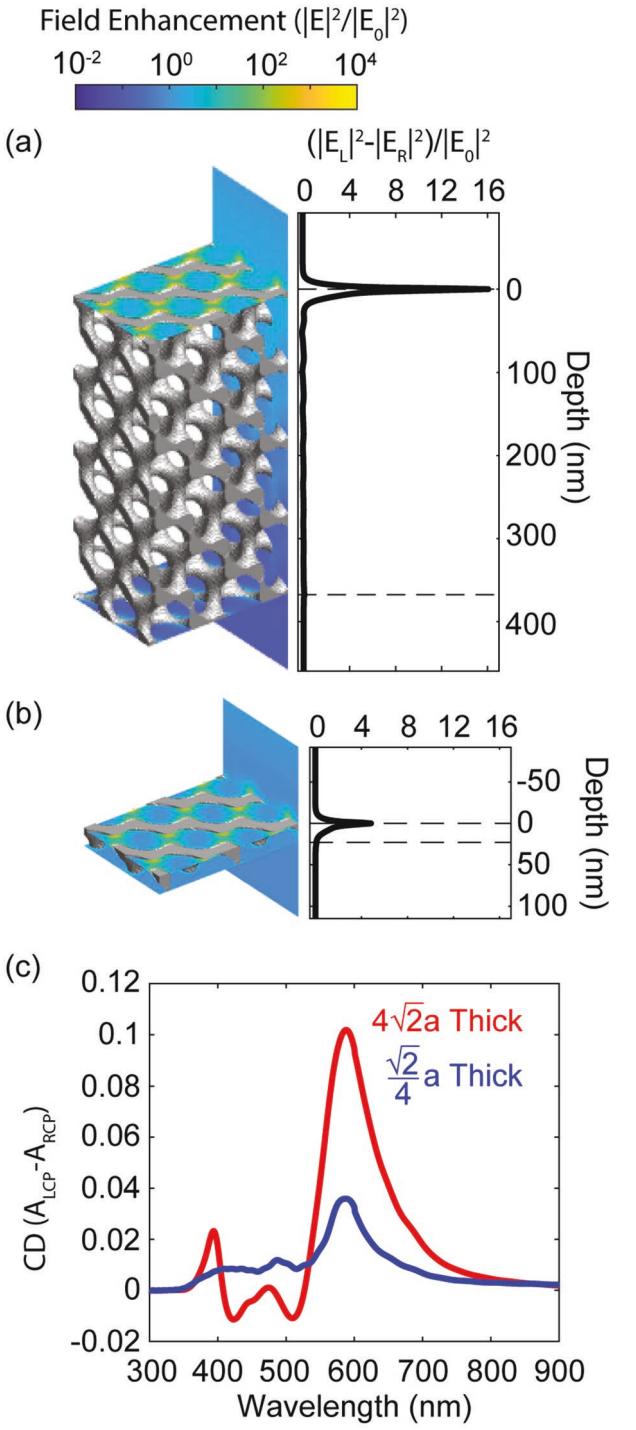

Figure 5. Local electric field enhancement and integrated difference in electric field intensity enhancement at the red-most CD resonance for [110] oriented positive ($m = +0.9$) single gyroid gyroids with a top termination at $\tau_{110} = 0.30$, $\lambda = 588$ nm, and a thickness of a) 368 nm ($4\sqrt{2}\,a$) or b) 23 nm ($\sqrt{2}/4a$). Dashed lines indicate the top and bottom termination planes. c) CD spectra from the gyroid metamaterial (full crystal) and the surface only.

that this metasurface structure is still a 3D structure, and is not a 2D extrusion of the surface geometry. Both single gyroids are [110] oriented, have a positive m value ($m = +0.9$), and have top

surface terminations at $\tau_{110} = 0.30$. The 23 nm thick gyroid has a bottom termination of $\tau_{110} = 0.80$ to avoid the excitation of surface resonances at the bottom face. The film and the 23 nm thick metasurface exhibit similar CD spectra, both supporting a positive CD peak at 588 nm. It is important to note that while the 368 nm thick metamaterial supports a larger CD magnitude, the 23 nm thick metasurface displays a higher level in selectivity with circularly polarized light as observed by a larger *g*-factor ($|g_{\text{metasurface}}| = 0.20$ vs $|g_{\text{metamaterial}}| = 0.16$).

The difference between the surface and bulk structures can be explained by the depth dependent cumulative absorption calculations and CD spectra of [110] oriented metamaterials of different thicknesses, shown in Figure S8 of the Supporting Information. Cumulative absorption calculations of the $4\sqrt{2}a$ thick metamaterial show that a majority of the absorption occurs within the top few nanometers of the top surface, but substantial, stepwise increases in absorption are also observed to occur every $\frac{\sqrt{2}}{2}a$ ($\Delta\tau_{110} = 1$) throughout the bulk of the crystal due to the interactions with the next set of chiral groups. The strength of the bulk interactions can therefore be tuned by varying the gyroid metamaterial's thickness in steps of $\frac{\sqrt{2}}{2}a$. The stepwise reintroduction of bulk interactions is shown in Figure S8b of the Supporting Information, which shows the CD spectra of [110] oriented, positive ($m = +0.9$) single gyroid metamaterials with top surface terminations of $\tau_{110} = 0.30$ and thicknesses varying from $0.25\sqrt{2}a$ to $3.75\sqrt{2}a$. These thicknesses were selected to generate bottom surface terminations of $\tau_{110} = 0.8$ and avoid the excitation of surface resonances on the bottom of the gyroid in the thinner samples. Substantial increases in the CD peak at ≈600 nm are observed as the thickness increases due to the increased total absorption within the system. The *g*-factor of the structure, shown in Figure S8c of the Supporting Information, decreased substantially from 0.2 to 0.15 when bulk contributions were first introduced (thickness increase from $0.25\sqrt{2}a$ to $0.75\sqrt{2}a$), but then stayed relatively constant as the gyroid further increased in thickness. Increasing the gyroid's thickness also causes the bulk generated CD in the 350–500 nm spectral range to emerge.

The influence of top and bottom surface resonances can also be tuned for gyroids oriented along the [111] direction by controlling the termination plane and metal infill percentage. **Figure 6**a,b shows the termination dependent CD spectra of [111] oriented positive ($m = +1.2$) and negative ($m = -1.2$) gyroid metamaterials with ≈10 vol% silver, which consist of a series of largely termination independent bands of CD peaks in the visible, and two interweaving, arcing bands of CD peaks in the NIR. Similar to the [100] direction, the [111] direction's termination dependent CD is symmetric every $\Delta\tau_{111} = 0.5$, and is primarily detected in transmission measurements (Figure S9, Supporting Information). A $\Delta\tau_{111} = 0.25$ shift in enantiomeric CD response in the positive and negative structures is observed by the particularly strong CD signal that occurs when the two interweaving bands of CD peaks intersect in the positive ($m = +1.2$) gyroid at $\tau_{111} = 0.375$ and 0.875 and in the negative ($m = -1.2$) gyroid at $\tau_{111} = 0.125$ and 0.625. This enantiomeric shift enables [111] oriented double gyroids to support CD signals, but the chiroptical response is weak due to spectral overlap of the CD peaks from the two single gyroids.

We interrogate the origin of these interweaving bands of CD peaks in the NIR by investigating the regions of largest electric field localization strength and selectivity. Figure 6c,d shows the field profiles and integrated difference in the electric field intensity enhancement of the [111] oriented positive ($m = +1.2$) gyroid at the red-most CD peaks for the (111) and (444) terminated gyroids. The [111] direction consists of layers of hexagonally packed triangular features connected by ⟨110⟩ struts. In $m = +1.2$ single gyroid networks, the (111) planes ($\tau_{111} = 0$) are located at the bottom of the triangular layers. Therefore, the top surface of a (111) terminated gyroid consists of a hexagonally packed trimer array while the bottom surface contains the triangular features. The preferential concentration of RCP illumination at the top surface in Figure 6c shows that it is this trimer array that is responsible for the red-shifted CD minimum. In comparison, (444) planes ($\tau_{111} = 0.25$) are located at the top of these triangular layers causing a (444) terminated gyroids to flip the location of the triangle and trimer arrays relative to those terminated at (111) planes. Here, the trimer arrays, and therefore the selective concentration of RCP illumination, are located at the bottom surface. These top and bottom surfaces resonances are simultaneously excited at the intersection of these CD peak bands, as shown for the $\tau_{111} = 0.125$ and $\tau_{111} = 0.375$ gyroids in Figure 6e,f. Increasing the fill fraction of Ag reduces the access to the bottom surface resonances. For [111] oriented single gyroids with ≈20 vol% Ag infill, the bottom surface resonances are significantly weaker than those on the top surface, due to the attenuation of light as it travels through the bulk of the gyroid (Figure S10, Supporting Information).

Moving off the principal crystallographic orientations can generate even stronger chiral optical behavior. The [211] direction is of particular interest for gyroid optical metamaterial development as it often preferentially orients normal to the substrate.[24–26] The termination dependent CD response of [211] oriented single gyroids is shown in Figure S11 of the Supporting Information. Similar to the [110] direction, [211] oriented single gyroids support termination independent CD peaks, detectable in transmittance measurements, that display the Cotton effect as well as a termination dependent CD signal, detectible in reflectance. However, in contrast to the [110] oriented single gyroids, [211] oriented positive ($m = +0.9$) and negative ($m = -0.9$) single gyroids are enantiomers of one another, displaying mirror symmetric CD for all termination groups between equivalent (211) planes with the maximum/minimum CD observed at a termination of $\tau_{211} = 0.78$ for both enantiomers.

Most notably, the *g*-factor for [211] oriented positive ($m = +0.9$) and negative ($m = -0.9$) single gyroid metamaterials (**Figure 7**a,b) is approximately twice that of any other single gyroid orientation investigated in this study. We can understand these large *g*-factors by investigating the local field enhancement and integrated difference in electric field intensity enhancement of the [211] oriented single gyroids at their *g*-factor maximum of $\tau_{211} = 0.78$ (Figure 7c–e). At this termination, the [211] oriented gyroids' top surface consists of a square array of "L" shaped structures whose handedness depends on the handedness of the gyroid network. The "L" shaped top surfaces strongly and selectively concentrate light of one circular

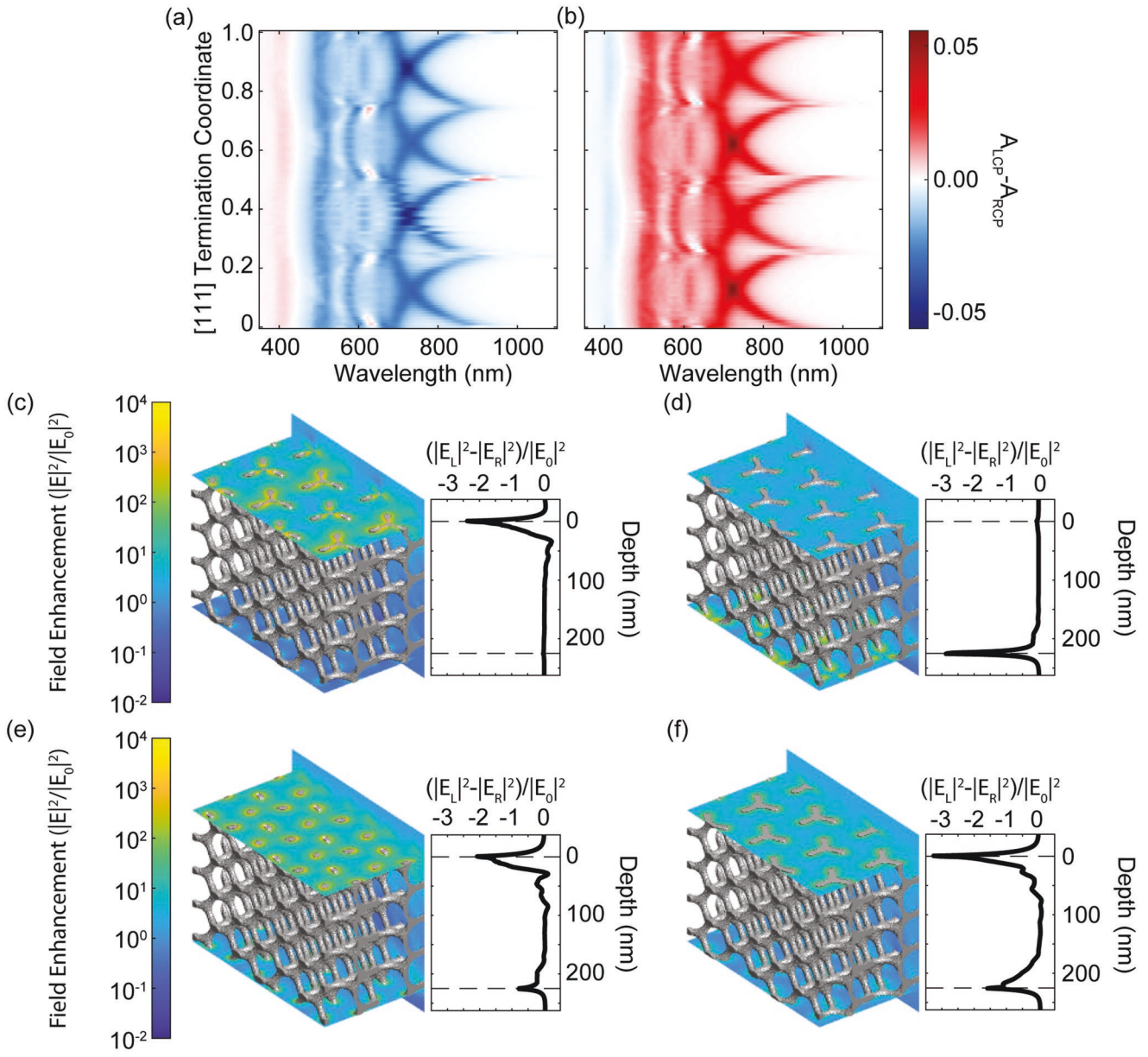

Figure 6. Termination resolved circular dichroism spectra for 225 nm thick ($2\sqrt{3}a$) [111] oriented a) positive ($m = +1.2$) and b) negative ($m = -1.2$) single gyroids. c–f) Local field enhancement and integrated difference in electric field intensity enhancement of the positive gyroids at their red-most CD wavelength: (c) $\tau_{111} = 0$ at $\lambda = 850$ nm, (d) $\tau_{111} = 0.25$ at $\lambda = 864$ nm, (e) $\tau_{111} = 0.125$ at $\lambda = 737$ nm, (f) $\tau_{111} = 0.375$ at $\lambda = 723$ nm. Dashed lines indicate the top and bottom termination planes.

polarization, as shown by the large difference in local field enhancement in the vicinity of the "L" shaped structures under left- and right-handed circularly polarized light.

In real devices, defects on the surface or in the bulk could alter the self-assembly templated gyroid metamaterial's optical response away from that of the perfect gyroid crystal CD. For example, surface roughness that exposes multiple termination groups or interrupts coupling between surface structures could result in significant changes between modeled and experimental CD spectra. Surface roughness could arise from transfer from a nonplanar substrate, from the block copolymer deposition and annealing steps, or nonuniform etching of the polymer and irregularities in the metal infilling. **Figure 8**a shows the termination resolved circular dichroism of a [110] oriented gyroid metamaterial with a 1 nm root mean squared (RMS) surface roughness on both top and bottom surfaces. Comparing this rough gyroid's termination dependent CD behavior to the perfect crystal in Figure 4a, we see that the introduction of surface roughness has no effect on the termination independent CD spectra generated from bulk interactions. The termination dependent surface resonances, however, are spread over a wider termination range. This remains true for gyroid metamaterials with levels of surface roughness on the order of typical block copolymer line edge roughnesses,[27,28] as shown by the 5 nm

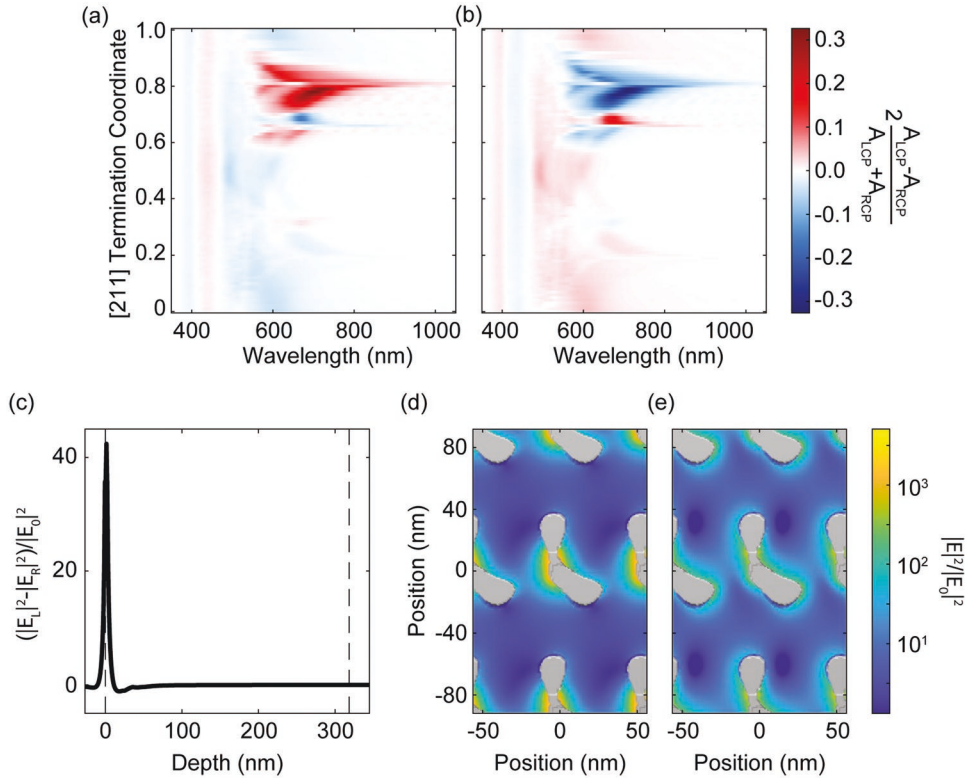

Figure 7. Termination resolved *g*-factors for 318 nm thick ($2\sqrt{6}a$) [211] oriented a) positive ($m = +0.9$) and b) negative ($m = -0.9$) single gyroid enantiomers. c) Integrated difference in electric field intensity enhancement for a positive [211] oriented, $\tau_{211} = 0.78$ single gyroid metamaterial at a wavelength of 700 nm. Dashed lines indicate the top and bottom termination planes. Electromagnetic field profile at the top surface of the positive $\tau_{211} = 0.78$ single gyroid metamaterial under 700 nm d) left- and e) right-handed circularly polarized illumination.

RMS rough gyroid metamaterial's [110] termination dependent CD in Figure S12a of the Supporting Information.

In addition to surface roughness defects, defects within the bulk of the crystal could disrupt the CD spectra. One potential defect is the incomplete connection of nodes by the ⟨110⟩ oriented struts.[29] This incomplete connection could arise during block copolymer self-assembly, or from to an incomplete metal infill. Figure 8b shows that there are negligible changes upon removing a strut along the [110] direction in the middle of a [110] oriented positive ($m = +0.9$) single gyroid metamaterial at a defect density of 4.55×10^{14} cm^{-3}. Surprisingly, the effect is still negligible when all of the [110] oriented struts are removed (see Figure S12b, Supporting Information). The [110] struts form a hexagonally packed cylinder arrangement in [110] oriented gyroids, as shown by the $\tau_{110} = 0.8$ surface schematic in Figure 4d. The depth dependent absorption calculations in Figure S8 of the Supporting Information show that the hexagonally packed cylinder arrangement only weakly interacts with the incident electromagnetic radiation, so removal of the [110] struts only slightly perturbs the system.

However, removal of struts along the other directions significantly impacts the gyroid's optical response. Removal of a [1$\bar{1}$0]

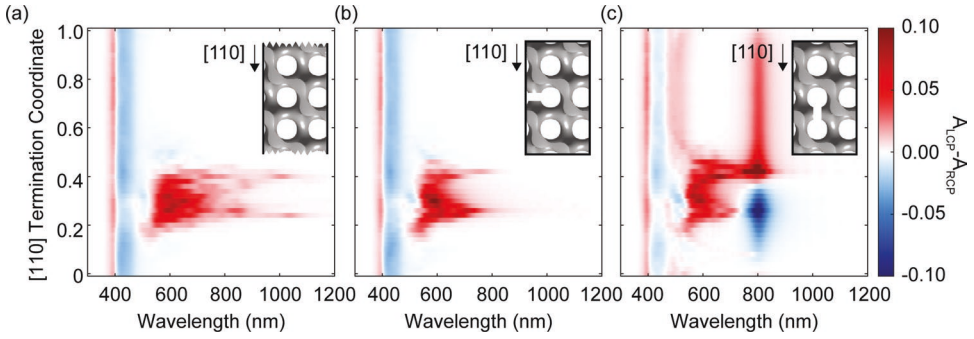

Figure 8. Termination resolved circular dichroism spectra for a 368 nm ($4\sqrt{2}a$) [110] oriented positive ($m = +0.9$) single gyroid metamaterial with various defects. a) 1 nm RMS surface roughness, b) removal of a [110] oriented strut, and c) removal of a [1$\bar{1}$0] oriented strut. Strut removal defect densities are at 1 strut removal per $\sqrt{2}a \times a \times 4\sqrt{2}a$ unit volume (4.55×10^{14} cm^{-3}).

strut (Figure 8c) significantly disrupts the termination independent, bulk CD spectrum and generates an additional CD signal at ≈800 nm whose handedness depends on the top surface termination group. Omission of the $[1\bar{1}0]$ strut disrupts the additional bulk absorption by the groups equivalent to those exposed on the surface between $\tau_{110} = 0.12$–0.44 in Figure 4d, which significantly alter the gyroid's far-field response. Decreasing the defect density to 5.06×10^{13} cm^{-3} (1 defect per $3\sqrt{2}a \times 3a \times 4\sqrt{2}a$ unit volume), results in a decrease in the defect's resonant strength, and a termination dependent CD response that more closely matches that of the perfect crystal as shown in Figure S12c of the Supporting Information.

3. Conclusion

In conclusion, the results presented in this report highlight the importance of controlling the gyroid metamaterial's crystallographic orientation, termination group, and infill conditions during fabrication as the far-field chiral optical response of a metal infilled gyroid metamaterial is dominated by resonances occurring at the top (or bottom) surfaces. In the [100] direction, resonances of thinly connected, "S" shaped tips generate strong, red-shifted CD spectral features. In the [110] direction, the separation of surface resonances between the two single gyroid networks allows double gyroids, which are achiral in the bulk, to support strong positive and negative CD spectral features depending on the exposed surface. Gyroid metamaterials are often dominated by top surface resonances, however, bottom surface resonances can be better obtained by decreasing the metal infill, as shown by a [111] oriented single gyroid with ≈10 vol% Ag infill. Moving off the principle crystallographic orientations can excite highly selective chiral surface resonances, as observed by the [211] single gyroids that support *g*-factors on the order of 0.33. The incorporation of various defects, both surface and bulk, can perturb the system in different ways. Surface roughness spreads out the termination dependent behavior over a wider range. Defects in [110] struts have negligible impact on the CD response of [110] gyroids due to low incoupling strength around the defect, while defects in the $[1\bar{1}0]$ struts significantly impact the overall optical response. Lastly, applications that utilize gyroid metamaterials in reflectance or transmittance will need to consider crystallographic orientation and design for bulk or surface driven CD. The CD signal of [100] and [111] oriented gyroids is detectable in transmittance, while [110] and [211] oriented gyroids will exhibit surface generated CD in reflectance and bulk CD in transmittance.

4. Experimental Section

The CD spectra of single and double gyroid metamaterials were evaluated using Lumerical FDTD simulations by illuminating the structure with both right- and left-handed circularly polarized light at normal incidence from the top. The absorbance of the structure under each incident polarization was calculated using the gyroid's reflectance and transmittance spectra: $A_{R/L} = 1 - R_{R/L} - T_{R/L}$. The optical response to unpolarized light was calculated by averaging of the left- and right-handed circularly polarized light simulation results

$$\left\langle |E|^2 \right\rangle = \frac{1}{2}|E_{LCP}|^2 + \frac{1}{2}|E_{RCP}|^2 \tag{3}$$

The gyroid network structures are defined using the following analytical equation for the gyroid's surface[30]

$$\sin(2\pi x/a)\cos(2\pi y/a) + \sin(2\pi y/a)\cos(2\pi z/a) + \sin(2\pi z/a)\cos(2\pi x/a) = m \tag{4}$$

where a is the periodicity of the gyroid, which is set to 65 nm in this study,[19,20] and m is a parameter such that $0 < |m| < \sqrt{2}$. The magnitude of m controls the volume fraction of the network domain. In this work, two different fill fractions are considered: $|m| = 0.9$, which generates single gyroid domains of approximately 20 vol%, and $|m| = 1.2$, which has a decreased fill fraction of ≈10 vol%. The sign of m is also used to determine the single gyroid network's handedness. Single gyroid networks described by a positive (negative) m value are defined as positive (negative) gyroids. The modeled gyroid metamaterials are assumed to consist of Ag networks in air, with the refractive index of Ag described by a Lorentz–Drude–Debye fit to complex refractive index data from Palik.[31]

To investigate all possible surface groups along a particular crystallographic direction, a termination coordinate, τ_{hkl}, is utilized in a manner similar to Dolan et al.[20] but expanded for use along any crystallographic direction within a cubic crystal system. The termination coordinate is defined as the distance from the crystallographic origin to the terminating plane along the direction of light propagation in units of structural periodicity, and is summarized by Equation (5)

$$\tau_{hkl} = \frac{x}{a}\sqrt{h^2 + k^2 + l^2} \tag{5}$$

where x is the distance from the plane (*hkl*) to the termination plane in the direction [*hkl*]. The termination coordinate is related to the corresponding, terminating Miller plane by dividing the orientation direction by the termination coordinate, as shown in Figure 1b,c. Termination coordinates of $\tau = 0$ and 1 are identical. For example, [100] oriented gyroids with $\tau_{100} = 0$ or 1 have (100) termination planes, a [110] oriented gyroid with $\tau_{110} = 0.5$ has (220) termination planes, and a [111] oriented gyroid with $\tau_{111} = 0.25$ has (444) termination planes. Unless otherwise stated, the thicknesses of the gyroid metamaterials are set to $4\sqrt{h^2 + k^2 + l^2}a$ for the [100] and [110] directions and $2\sqrt{h^2 + k^2 + l^2}a$ for the [111] and [211] directions. These thicknesses are selected to enable observation of both the surface and bulk driven chiral optical properties of gyroid metamaterials in thin film form, and have identical termination planes on the top and bottom surfaces.

Supporting Information

Supporting Information is available from the Wiley Online Library or from the author.

Acknowledgements

The authors thank Dr. Mahesh Mahanthappa, Dr. Jinwoo Oh, and Szu-Ming Yang for helpful scientific discussions. The authors also thank Lisa Zeeb for their assistance in figure design. This work was supported primarily by the National Science Foundation through the University of Minnesota MRSEC under Award No. DMR-2011401. The authors acknowledge the Minnesota Supercomputing Institute (MSI) at the University of Minnesota for providing resources that contributed to the research results reported within this paper.

Conflict of Interest

The authors declare no conflict of interest.

Data Availability Statement

The data that support the findings of this study are available from the corresponding author upon reasonable request.

Keywords

chirality, circular dichroism, metamaterials

Received: February 15, 2022
Revised: April 11, 2022
Published online: May 29, 2022

[1] J. A. Dolan, B. D. Wilts, S. Vignolini, J. J. Baumberg, U. Steiner, T. D. Wilkinson, *Adv. Opt. Mater.* **2015**, *3*, 12.
[2] E. Goi, B. P. Cumming, M. Gu, *Adv. Opt. Mater.* **2018**, *6*, 1800485.
[3] J. Lequieu, T. Quah, K. T. Delaney, G. H. Fredrickson, *ACS Macro Lett.* **2020**, *9*, 1074.
[4] L. Lu, L. Fu, J. D. Joannopoulos, M. Soljačić, *Nat. Photonics* **2013**, *7*, 294.
[5] K. Michielsen, D. G. Stavenga, *J. R. Soc., Interface* **2008**, *5*, 85.
[6] V. Saranathan, C. O. Osuji, S. G. J. Mochrie, H. Noh, S. Narayanan, A. Sandy, E. R. Dufresne, R. O. Prum, *Proc. Natl. Acad. Sci. USA* **2010**, *107*, 11676.
[7] G. E. Schröder-Turk, S. Wickham, H. Averdunk, F. Brink, J. D. Fitz Gerald, L. Poladian, M. C. J. Large, S. T. Hyde, *J. Struct. Biol.* **2011**, *174*, 290.
[8] V. Saranathan, S. Narayanan, A. Sandy, E. R. Dufresne, R. O. Prum, *Proc. Natl. Acad. Sci. USA* **2021**, *118*, 2101357118.
[9] Z. Almsherqi, F. Margadant, Y. Deng, *Interface Focus* **2012**, *2*, 539.
[10] W. Kuhn, *Annu. Rev. Phys. Chem.* **1958**, *9*, 417.
[11] J. K. Gansel, M. Thiel, M. S. Rill, M. Decker, K. Bade, V. Saile, G. von Freymann, S. Linden, M. Wegener, *Science* **2009**, *325*, 1513.
[12] M. Decker, R. Zhao, C. M. Soukoulis, S. Linden, M. Wegener, *Opt. Lett.* **2010**, *35*, 1593.
[13] A. Alvarez-Fernandez, C. Cummins, M. Saba, U. Steiner, G. Fleury, V. Ponsinet, S. B. Guldin, *Adv. Opt. Mater.* **2021**, *9*, 2100175.
[14] M. Stefik, S. Guldin, S. Vignolini, U. Wiesner, U. B. Steiner, *Chem. Soc. Rev.* **2015**, *44*, 5076.
[15] R. Dehmel, J. A. Dolan, Y. Gu, U. Wiesner, T. D. Wilkinson, J. J. Baumberg, U. Steiner, B. D. Wilts, I. Gunkel, *Macromolecules* **2017**, *50*, 6255.
[16] S. N. Abdollahi, E. Ochoa Martínez, C. Kilchoer, G. Kremer, T. Jaouen, P. Aebi, T. Hellmann, T. Mayer, Y. Gu, U. B. Wiesner, U. Steiner, B. D. Wilts, *Adv. Mater. Interfaces* **2020**, *7*, 2001227.
[17] K. Hur, Y. Francescato, V. Giannini, S. A. Maier, R. G. Hennig, U. Wiesner, *Angew. Chem., Int. Ed.* **2011**, *50*, 11985.
[18] S. S. Oh, A. Demetriadou, S. Wuestner, O. Hess, *Adv. Mater.* **2013**, *25*, 612.
[19] C. Kilchoer, N. Abdollahi, J. A. Dolan, D. Abdelrahman, M. Saba, U. Wiesner, U. Steiner, I. Gunkel, B. D. Wilts, *Adv. Opt. Mater.* **2020**, *8*, 1902131.
[20] J. A. Dolan, R. Dehmel, A. Demetriadou, Y. Gu, U. Wiesner, T. D. Wilkinson, I. Gunkel, O. Hess, J. J. Baumberg, U. Steiner, M. Saba, B. D. Wilts, *Adv. Mater.* **2019**, *31*, 1803478.
[21] M. Saba, B. D. Wilts, J. Hielscher, G. E. Schröder-Turk, *Mater. Today Proc.* **2014**, *1*, 193.
[22] M. L. Solomon, J. Hu, M. Lawrence, A. García-Etxarri, J. A. Dionne, *ACS Photonics* **2019**, *6*, 43.
[23] Z. Wang, F. Cheng, T. Winsor, Y. Liu, *Nanotechnology* **2016**, *27*, 412001.
[24] S. R. Nowak, K. K. Lachmayr, K. G. Yager, L. R. Sita, *Angew. Chem., Int. Ed.* **2021**, *60*, 8710.
[25] M. P. Tate, V. N. Urade, S. J. Gaik, C. P. Muzzillo, H. W. Hillhouse, *Langmuir* **2010**, *26*, 4357.
[26] V. N. Urade, T.-C. Wei, M. P. Tate, J. D. Kowalski, H. W. Hillhouse, *Chem. Mater.* **2007**, *19*, 768.
[27] R. Ruiz, L. Wan, R. Lopez, T. R. Albrecht, *Macromolecules* **2017**, *50*, 1037.
[28] K. S. Lee, J. Lee, J. Kwak, H. C. Moon, J. K. Kim, *ACS Appl. Mater. Interfaces* **2017**, *9*, 31245.
[29] X. Feng, H. Guo, E. L. Thomas, *Polymer* **2019**, *168*, 44.
[30] K. Michielsen, J. S. Kole, *Phys. Rev. B* **2003**, *68*, 115107.
[31] E. D. Palik, *Handbook of Optical Constants of Solids*, Academic Press, San Diego **1998**, pp. 350–357.